



BERNARDO ONÇA PRESTES

**Recente dispersão através do Rio Amazonas promoveu forte isolamento genético
no Formigueiro-ferrugem *Myrmoderus ferrugineus* (Aves: Thamnophilidae)**

BERNARDO ONÇA PRESTES

**Recente dispersão através do Rio Amazonas promoveu forte isolamento genético
no Formigueiro-ferrugem *Myrmoderus ferrugineus* (Aves: Thamnophilidae)**

Dissertação apresentada ao Programa de Pós-Graduação em Zoologia, do convênio da Universidade Federal do Pará e Museu Paraense Emílio Goeldi, como requisito parcial para obtenção do título de Mestre em Zoologia.

Área de concentração: Evolução

Linha de Pesquisa: Biogeografia e Filogeografia.

Orientador: Dr. Pedro Peloso
Co orientador: Ph.D. Alexandre Aleixo

Belém, 2018

Dados Internacionais de Catalogação na Publicação
(CIP) Sistema de Bibliotecas da Universidade Federal
do Pará

Gerada automaticamente pelo módulo Ficat, mediante os dados fornecidos pelo(a)
autor(a)

P936r

Prestes, Bernardo Onça

Recente dispersão através do Rio Amazonas promoveu forte isolamento genético no
Formigueiro- ferrugem *Myrmoderus ferrugineus* (AVES: THAMNOPHILIDAE) / Bernardo Onça
Prestes, Pedro Luiz Vieira Del Peloso. — 2018
30 f. : il. color

Dissertação (Mestrado) - Programa de Pós-graduação em Zoologia (PPGZOO), Instituto de
Ciências Biológicas, Universidade Federal do Pará, Belém, 2018.

Orientação: Prof. Dr. Pedro Luiz Vieira Del Peloso

Coorientação: Prof. Dr. Alexandre Luis Padovan

Aleixo.

1. Amazônia. 2. Biogeografia. 3. Captura de drenagem. 4. Holoceno. 5. Pleistoceno tardio. I.
Peloso, Pedro Luiz Vieira Del. II. Peloso, Pedro Luiz Vieira Del, *orient.* III. Título

FOLHA DE APROVAÇÃO

BERNARDO ONÇA PRESTES

Recente dispersão através do Rio Amazonas promoveu forte isolamento genético no Formigueiro-ferrugem *Myrmoderus ferrugineus* (Aves: Thamnophilidae)

Tese/Dissertação apresentada ao Programa de Pós-Graduação em Zoologia, do convênio da Universidade Federal do Pará e Museu Paraense Emílio Goeldi, como requisito parcial para obtenção do título de Mestre em Zoologia, sendo a COMISSÃO JULGADORA composta pelos seguintes membros:

Dr. Marcos Pérsio Dantas Santos

Universidade Federal do Pará

Dra. Camila Cherem Ribas

Instituto Nacional de Pesquisas da Amazônia

Dr. Renato Caparroz

Universidade de Brasília

Dr. Fabio Sarubbi Raposo do Amaral

Universidade Federal de São Paulo

Dr. Péricles Sena do Rêgo

Universidade Federal do Pará

Aprovada em: 02 de abril de 2018

Local de defesa: Museu Paraense Emílio Goeldi

À Antônio Onça e Maria Onça,
meu eterno amor.

“Nada como um dia após o outro dia”
(Racionais MC's)

AGRADECIMENTOS

À Universidade Federal do Pará pela oportunidade de cursar uma Pós-Graduação.

À minha família pela estruturação e ensinamentos. Pelos bons e maus momentos. Obrigado por tudo!

Para Antônio e Maria, meu eterno amor!

José e Raimunda, meu amor também é de vocês.

Aos meus irmãos Yuri, Vinícius e Maricília, pelos 25 anos de convivência e amizade.

À minha princesa, Larissa. Sou o homem mais sortudo do mundo por lhe ter como companheira. Que eu lhe faça muito feliz também. Obrigado por tudo!

Aos amigos do Mestrado, pelos anos de aprendizado e parceria, que a partir de agora seja só sucesso!

Ao orientador Pedro Peloso, por todo o conhecimento e aprendizado durante esses dois anos. Agradeço a oportunidade de ter vivenciado esses momentos. Obrigado por tudo.

Ao co-orientador Alexandre Aleixo por todos esses anos de convivência. Obrigado pelos aprendizados e por abrir as portas do MPEG para que pudesse fazer parte da família Goeldi.

À Aline pelo processo de sequenciamento das amostras.

À Sofia, por ter me ajudado bastante na execução das análises e discussão dos resultados. E por sempre estar disposta a ajudar. Você é demais!

Ao pessoal do laboratório, pelos momentos de risadas e aprendizado. Assim como todos que um dia ajudaram na minha construção. Vocês sempre serão lembrados!

SUMÁRIO

ABSTRACT	8
RESUMO	9
INTRODUCTION	10
METHODS	13
Samplig.....	13
Phylogenetic analysis	13
Population genetics.....	14
RESULTS	15
Data characteristics.....	15
Phylogenetic analysis	16
Population structure, gene flow and demography	18
DISCUSSION	20
Intraspecific relationships in <i>M. ferrugineus</i>	20
The Amazon as a barrier to geneflow for antbirds	21
A recent dispersal across the Amazon River explains <i>M. ferrugineus</i> phylogeographic structure	22
REFERENCES	24
APPENDIX	28
Appendix S1	28
Appendix S2	30

Recent dispersal across the Amazon River promoted strong genetic isolation in the Ferruginous-backed Antbird *Myrmoderus ferrugineus* (Aves: Thamnophilidae)

ABSTRACT

One of the most debated hypotheses to explain the origin of such a rich Amazonian biota is the "river-barrier" hypothesis, which advocates that main Amazonian rivers acted as powerful barriers promoting isolation and species diversification. Herein, we used an statistical phylogeography approach to study the Ferruginous-backed Antbird species *Myrmoderus ferrugineus*, an Amazonian upland terra-firme forest endemic species with two known morphologically little differentiated subspecies separated by the mid-Amazon River (*M. f. ferrugineus* and *M. f. elutus*). We used the phylogeographic data to address the following alternative scenarios of diversification for *M. ferrugineus*: 1) the Amazon River does not coincide with major phylogeographic breaks separating *M. ferrugineus* populations; 2) the Amazon River is correlated with ancient phylogeographic structure within *M. ferrugineus*, probably resulting from the river's establishment during the Plio-Pleistocene or before that; and 3) the Amazon River correlates with a recent divergence between *M. ferrugineus* populations, probably due to recent dispersal and isolation after the river's establishment during the Plio-Pleistocene. We sequenced 2 MtDNA and 2 nuclear genes from 13 individuals of *M. f. ferrugineus* and 15 individuals of *M. f. elutus* to estimate concatenated and time-calibrated coalescent multilocus phylogenies. We also tested for the occurrence of past population bottlenecks, gene flow and effective population size fluctuations in *M. f. ferrugineus* and *M. f. elutus*. Our results retrieved with strong statistical support the monophyly between *M. f. ferrugineus* and *M. f. elutus*, and pointed to a scenario of strong population structure and absence of gene flow between these subspecies. However, according to two independent coalescent dating methods, *M. f. ferrugineus* and *M. f. elutus* diverged between 2.5 and 75,000 years ago, therefore well after the modern establishment of the Amazon River. Our results demonstrate that even upland terra-firme forest taxa with low dispersal abilities such as antbirds, have been able to establish populations across the Amazon River after its modern course became established. Whether these events were caused by active or passive dispersal mediated by drainage capture events remain to be determined, although the second scenario is more likely considering the Ferruginous-backed Antbird ecological attributes. Therefore, we anticipate that important drainage capture events involving the middle Amazon River course could have taken place between the Late Pleistocene and as recent as the Holocene, favoring the crossing of several lineages previously isolated on opposite river banks.

Keywords: Amazonia, biogeography, drainage capture, Holocene, Late Pleistocene.

**Recente dispersão através do Rio Amazonas promovendo forte isolamento genética em
Formigueiro-ferrugem (*Myrmoderus ferrugineus*)**

RESUMO

Uma das hipóteses mais discutidas para explicar a origem de uma biota amazônica tão rica, é a hipótese dos "rios como barreira", referindo-se à atuação dos principais rios amazônicos como barreira promotora do isolamento e diversificação das espécies. Utilizamos abordagem de filogeografia estatística para estudar a espécie de *Myrmoderus ferrugineus*, espécie amazônica endêmica de florestas terra-firme com duas subespécies morfologicamente pouco diferenciadas e separadas pelo rio Amazonas (*M. f. ferrugineus* e *M. f. elutus*). Usamos dados filogeográficos para abordar os cenários de diversificação em *M. ferrugineus*: 1) o rio Amazonas não coincide com as grandes rupturas filogeográficas que separaram as populações de *M. ferrugineus*; 2) o rio Amazonas está correlacionado com a antiga estruturação filogeográfica dentro de *M. ferrugineus*, provavelmente resultante do estabelecimento do rio durante o Plio-Pleistoceno ou antes disso; e 3) o rio Amazonas correlaciona-se com uma divergência recente entre as populações de *M. ferrugineus*, provavelmente devido à dispersão e isolamento recente após o estabelecimento do rio durante o Plio-Pleistoceno. Sequenciamos 2 genes mitocondriais e 2 genes nucleares de 13 indivíduos de *M. f. ferrugineus* e 15 indivíduos de *M. f. elutus* para estimar filogenias concatenadas e *multilocus* coalescentes temporalmente calibradas. Testamos a ocorrência de *bottlenecks* na população passada, fluxo gênico e flutuações no tamanho efetivo populacional em *M. f. ferrugineus* e *M. f. elutus*. Nossos resultados recuperaram com um forte apoio estatístico para monofilia entre *M. f. ferrugineus* e *M. f. elutus*, seguido de forte estruturação populacional e ausência de fluxo gênico entre as subespécies. Porém, segundo os dois métodos independentes de datação coalescente, *M. f. ferrugineus* e *M. f. elutus* divergiram entre 2,5 e 75.000 anos atrás, bem depois do estabelecimento moderno para o rio Amazonas. Nossos resultados demonstraram que até mesmo táxons de florestas de terra firme com baixas habilidades de dispersão, como os Papa-formigas, foram capazes de estabelecer populações através do rio Amazonas depois de seu curso moderno ter se estabelecido. Se esse evento foi causado por dispersão ativa ou passiva mediada por eventos de captura de drenagem permanecem por incertos, embora o segundo cenário seja mais provável, considerando os atributos ecológicos da espécie. Antecipamos que eventos importantes de captura de drenagem envolvendo o curso médio do rio Amazonas poderiam ter ocorrido entre o Pleistoceno tardio até o Holoceno recente, favorecendo o cruzamento de várias linhagens previamente isoladas em bancos de rios opostos.

Palavras-chave: Amazônia, biogeografia, captura de drenagem, Holoceno, Pleistoceno tardio.

INTRODUCTION

The Neotropical region is characterized by its abundant fauna and flora, and by the complex evolutionary scenarios that helped shape today's local biota (Hoorn et al., 2010; Smith et al., 2014). The dynamic complexity of Amazonian ecosystems has puzzled biogeographers for many decades, and studies aiming to understand the distribution patterns and processes in Amazonia stem from the early observations of Alfred R. Wallace (Wallace, 1854). In what is now widely known as the *riverine barrier hypothesis* Wallace originally observed that many Amazonian species have their distributions limited by major rivers. Although there are many exceptions to this general pattern, most Amazonian rivers significantly reduce or prevent gene flow between populations of multiple organisms inhabiting opposite river banks, hence promoting allopatric speciation or at least preventing contact between closely related taxa (Aleixo, 2004; Antonelli et al., 2009; Ribas et al., 2012; Smith et al., 2014; Alfaro et al., 2015; Gibbs et al., 2018). Not surprisingly, the major Amazonian rivers are focus of much of the attention given in biogeographic studies in the Amazon basin.

The Amazon River is the largest river of South America and forms the largest drainage system in the World, both in terms of the volume of water flow, and the area covered by its basin (Milliman, 2001). The River, which divides the Amazonian rainforest in two major blocks (a northern and a southern one), has its origin in the Peruvian Andes, then flows through the Brazilian Amazonian lowlands and empties into the Atlantic Ocean—a journey of over 5,000 km. Moreover, the River is considered the strongest and most consistently effective geographical barrier among all the different rivers that compose the Amazon Basin (Hoorn et al., 2010). However, despite the progress made by studies on paleogeography, paleobiography and paleoecology, the dating for the formation of the Amazon river is still controversial (Campbell et al., 2006; Hoorn et al., 2010; Latrubesse et al., 2010; Gibbs et al., 2018). Here, we use the Ferruginous-backed Antbird *Myrmoderus ferrugineus* (Aves: Thamnophilidae) as a model to test the effects of the Amazon River as a barrier to gene flow and as a promoter of diversification among lineages of upland *terra firme* forest.

Myrmoderus ferrugineus is a small-sized (14–15 cm, 24–29 g), common, yet elusive, Antbird found in the understory of humid *terra firme* forest—sometimes it may also be observed in creek-side and tall white-sand forests known in Brazil as *campinaranas*. Two morphologically little differentiated subspecies are currently recognized: *M. ferrugineus ferrugineus* (Statius Muller, 1776)—distributed exclusively north of the Amazon River on the eastern part of the Guiana shield; and *M. ferrugineus elutus* (Todd, 1927)—distributed exclusively south of the Amazon river between the Madeira and Tapajós rivers (Zimmer & Isler, 2003). Phenotypically, *M. ferrugineus elutus* has more white on the upper belly and paler underparts than the nominate subspecies (Todd, 1927). Also, song and calls of both subspecies are also very similar, although some differences in peak frequency and pace might also consistently separate them. These minor phenotypic differences contrast with

those observed for other avian taxa separated by the Amazon River, where phenotypic and genetic divergences across the Amazon are high (Ribas et al. 2012, Sousa-Neves et al. 2013); alternatively, it is possible that *M. ferrugineus ferrugineus* and *M. ferrugineus elutus* are morphologically distinct cryptic species as also documented for several other antbird taxa separated by high genetic distances across Amazonian rivers (Fernandes et al. 2012, 2014; Thom and Aleixo 2015). Given the distribution of *M. ferrugineus ferrugineus* and *M. ferrugineus elutus* across the Amazon River (Figure 1), and the low levels of phenotypic divergences between, we chose these taxa to tackle questions related to the barrier effect of the Amazon River on upland terra-firme forest populations.

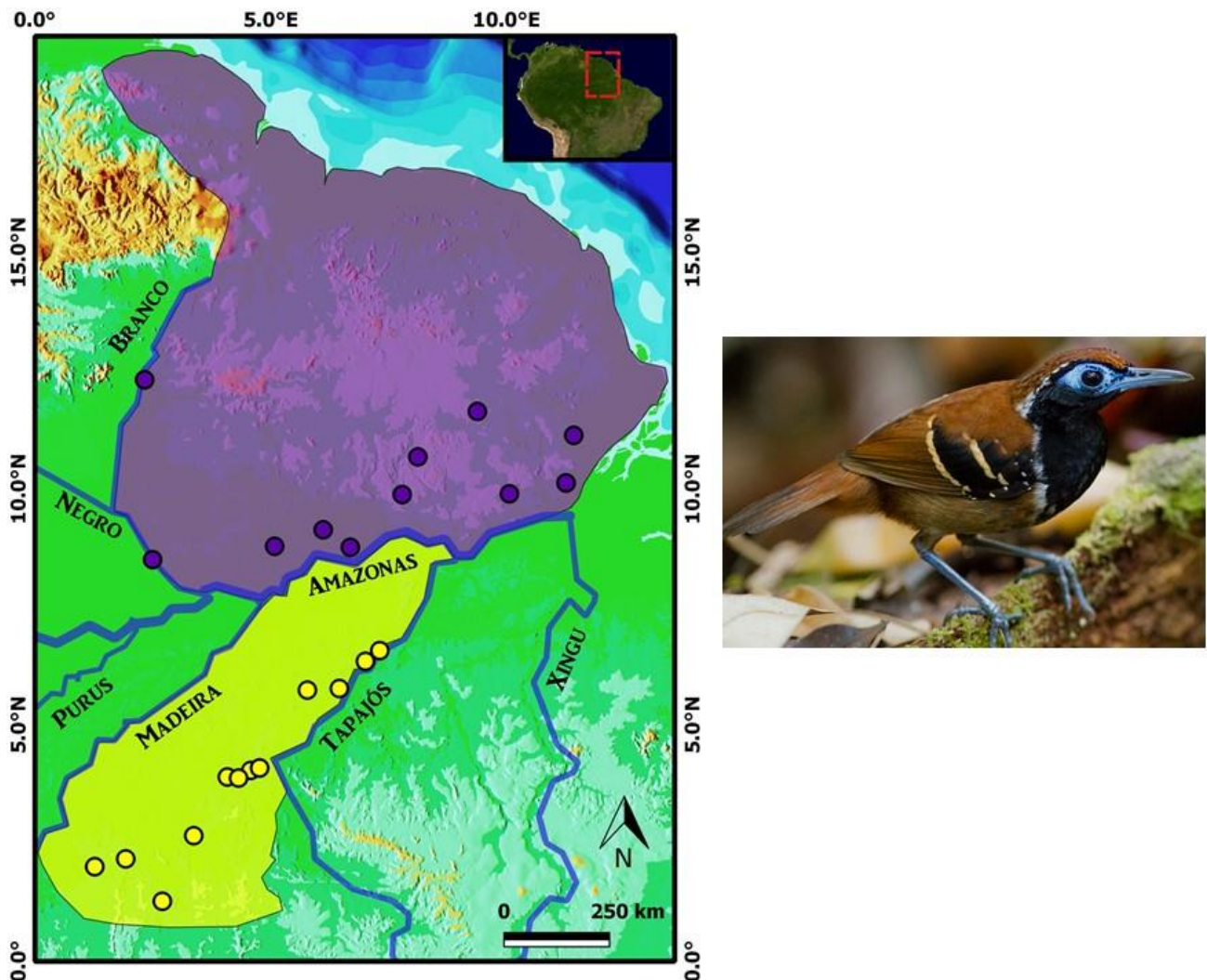


Figure 1 Geographical ranges and samples included in the study (circles) of the two subspecies of Ferruginous-backed Antbird. *Myrmoderus ferrugineus ferrugineus* (purple range and dots, northern distribution, shown in the photo); *M. f. elutus* (yellow range and dots, southern distribution). Photo by Pablo Cerqueira.

We used *M. ferrugineus* to test the potential role of the Amazon River as a barrier according to the river hypothesis proposed by Wallace (1854). More specifically, we used phylogeographic data

to address the following alternative scenarios of diversification for *M. ferrugineus*, derived from their overall great plumage similarities across the Amazon River: 1) the Amazon River does not coincide with major phylogeographic breaks separating *M. ferrugineus* populations; 2) the Amazon River is correlated with ancient phylogeographic structure within *M. ferrugineus*, probably resulting from the river's establishment during the Plio-Pleistocene or before that; and 3) the Amazon River correlates with a recent divergence between *M. ferrugineus* populations, probably due to recent dispersal and isolation after the river's establishment during the Plio-Pleistocene (Table 1). To this end, we carried out multi-locus phylogeographic and population genetics analyzes to study the divergence patterns between the two subspecies.

Table 1. Assumptions and phylogeographic and populations genetics predictions of the main scenarios of diversification evaluated in the present study.

Scenario	Prediction
H ₀ - The Amazon river is not barrier	There is a lack of phylogeographic structure (no reciprocal monophyly) and widespread geneflow between northern and southern populations.
H ₁ - The Amazon River is correlated with ancient (Plio-Pleistocene) phylogeographic structure within <i>M. ferrugineus</i>	There is phylogenetic structure (reciprocal monophyly) but only very limited (or none) gene flow between northern and southern populations. In addition to monophyly, timing of cladogenesis is concordant with the river's establishment during the Plio-Pleistocene or before that. The establishment of the Amazon River would have occurred around 7 million years ago (Mya) for Hoorn et al. (2010), between 6 and 5 Mya for Campbel et al. (2006) and 2,5 Mya for Latrubesse et al. (2010).
H ₂ - The Amazon River correlates with a recent divergence between <i>M. ferrugineus</i> populations	There is phylogenetic structure (reciprocal monophyly) but only very limited (or none) gene flow between northern and southern populations. Despite monophyly, timing of cladogenesis is more recent than river's the establishment during the Plio-Pleistocene or before that. The establishment of the Amazon River would have occurred around 7 million years ago (Mya) for Hoorn et al. (2010), between 6 and 5 Mya for Campbel et al. (2006) and 2,5 Mya for Latrubesse et al. (2010).

METHODS

Sampling

Our sample consisted of 28 individuals of *M. ferrugineus* (13 corresponding to *M. f. ferrugineus* and 15 to *M. f. elutus*) significantly covering its area of distribution (Fig. 1). We also included individuals of Squamate Antbird (*Myrmoderus squamosus*), Scalloped Antbird (*Myrmoderus ruficaudus*), White-bibbed Antbird (*Myrmoderus loricatus*) and Cordillera Azul Antbird (*Myrmoderus eowilsoni*) as outgroup terminals, following previous studies suggesting that the genus *Myrmoderus* is monophyletic (Isler et al. 2013; Moncrieff et al., 2018) (Appendix S1). Tissue samples were obtained from Instituto Nacional de Pesquisas da Amazônia, Brazil (INPA), Museu Paraense Emilio Goeldi, Brazil (MPEG), and Museu de Zoologia da Universidade de São Paulo, Brazil (MZUSP).

Total genomic DNA was extracted and isolated from tissue samples using the DNeasy Qiagen kit (Hilden, Germany), following the manufacturer's manual. Two mitochondrial genes (*Cytochrome B*, CYTB and *NADH Dehydrogenase Subunit 2*, ND2) and two nuclear genes (*Glyceraldehyde 3-phosphate Dehydrogenase Intron 11*, G3PDH and *Muscle Skeletal Receptor Tyrosine Kinase*, MUSK) were amplified via Polymerase Chain Reaction (PCR). Amplifications were performed in 12.5µl volumes, containing 1.25µl 10x reaction buffer, 1.5mM MgCl₂, 0.4mM each dNTP, 0.2µM each primer, 1 unit of Taq DNA polymerase (Invitrogen) and 10 – 25 ng of genomic DNA. Thermal cycling conditions for ND2 and G3PDH markers were an initial denaturation step of 95 °C for 5 min, followed by 35 cycles of 95 °C (1 m), 59 °C for ND2 and 65 °C for G3PDH (45 s), 72 °C (1 m), and a final extension step of 72 °C of 7 min. Touchdown cycling parameters, differing only in annealing temperatures, was used for CYTB and MUSK with 50 °C for four cycles, 49 °C for four cycles, 48 °C for 35 cycles. Amplification products were cleaned with PEG8000 filtered and cycle-sequenced using a Big Dye Terminator v3.01 kit following supplier orientation (Applied Biosystems). Primers used for PCRs and sequencing reactions are given in Appendix S2.

Both DNA strands were assembled in contigs, and sequences were inspected and corrected using BioEdit 7.0.5.3 (Hall, 1999). Heterozygous and ambiguous positions were coded according to the IUPAC code.

Phylogenetic analysis

We aligned sequences in ClustalW (Thompson et al., 1994) using default parameters. Allelic phases were determined using PHASE 2.1.1 (Stephens & Scheet, 2005; Stephens et al., 2001). The evolutionary models used in downstream phylogenetic analyses were selected with PartitionFinder 1.1.1 (Lanfear et al., 2012) using the Akaike information criterion (AIC). We then performed a Bayesian inference analysis, as implemented in MrBayes 3.2.2 (Ronquist et al., 2012) using the four

genes obtained for the study (ND2, CYTB, G3PDH and MUSK). Four parallel simultaneous runs were performed, for a total of 50 million generations, with trees sampled every 10000 generations. This phylogeny was used as a guide tree to further test species and subspecies boundaries based on multilocus coalescent methods. We used the phylogroups that were genetically differentiated in the Bayesian tree.

For a species trees reconstruction, we used both nuclear and mtDNA genes in BEAST 1.7 (Drummond & Rambaut, 2007)— substitution models fitting each locus were the same used in the previous analysis. We applied the CYTB mutational rate of 2.1% sequence divergence per lineage per million years (following Weir & Schluter, 2008) in an uncorrelated lognormal relaxed clock. We unlinked substitution model parameters for each gene. Two independent runs of 50 million generations were performed sampling trees every 10000 generations. The convergence for all parameters in species trees and concatenated was assessed by evaluating stationarity of the Markov chain using TRACER v. 1.5 (Rambaut & Drummond, 2007). The maximum clade credibility trees were computed with TreeAnnotator (part of the BEAST package). The consensus tree was visualized in FigTree 1.2.3 (<http://tree.bio.ed.ac.uk/software/figtree/>).

Population Genetics

The genealogical relationships among individuals of each sequenced gene were visualized and haplotype networks were constructed in PopART 4.5.1.0 (Leigh & Bryant, 2015) based on the topologies recovered in the concatenated tree. Mean pairwise p-distances (Nei, 1987) within and among populations were calculated using all markers in MEGA 7.0 (Kumar et al., 2015). Nucleotide diversity (μ), haplotype diversity (Hd), number of haplotypes (h) and number of segregating sites (S) were calculated for each marker and subspecies. The neutrality test indexes Tajima's D (Tajima, 1989) and Fu's Fs (Fu, 1997) were also applied. All tests and simulations were conducted with DNAsp 5 (Librado & Rozas, 2009).

We used the isolation–migration model (Hey & Nielsen, 2004; Nielsen & Wakeley, 2001) implemented in IMA2 (Hey, 2009) to estimate the timing of subspecies divergence and to determine whether gene flow has occurred subsequently. Units of analysis were selected based on the phylogenetic analysis, which recovered each of subspecies as a separate clade.

We used the complete sequences of both mtDNA and nDNA genes sequenced. The HKY model (Hasegawa et al., 1985) was applied for all markers; an inheritance scale of 0.25 for the mtDNA and 1 for nDNA. We applied the CYTB mutational rate of 2.1% sequence divergence per lineage per million years (Weir & Schluter, 2008). Several runs were performed to establish the best priors for effective population sizes and migration parameters. The final run was performed using 10 000 generations as burn-in, with 100 000 trees sampled during 100 generations and use of 20 chains.

Lastly, the reconstructions of population sizes through time were performed under an Extended Bayesian Skyline Plot (EBSP) approach (Heled & Drummond, 2008) implemented in BEAST 1.8 (Drummond et al., 2012). The best fit substitution model for each marker, the substitution rates, priors and the MCMC run strategy were the same as described above for the other Bayesian phylogenetic analyses performed.

RESULTS

Data characteristics

Aligned DNA sequence database consists of a total of 3051 bp: CYTB (1096 bp), ND2 (1029 bp), G3PDH (406 bp) and MUSK (520 bp). The diversity statistics, and results of neutrality tests Tajima's D (Tajima, 1989) and Fu's F_s (Fu, 1997) are shown in Table 2.

Table 2 Population variation estimates and neutrality tests for each marker separated by *M. f. ferrugineus* and *M. f. elutus*. Values given in bold are significant at $P < 0.05$.

Lineage/Locus	S	k	π	h	Hd	F_s	D
<i>M. f. ferrugineus</i>							
CYTB	23	4.615	0.009	5	0.692	2.201	-1.630
ND2	14	2.956	0.003	8	0.956	-3.607*	-1.845*
G3PDH	120	10.109	0.025	8	0.723	5.120*	-2.697*
MUSK	4	1.298	0.003	6	0.717	-1.076	0.638
<i>M. f. elutus</i>							
CYTB	14	3.141	0.003	11	0.974	-6.871	-1.463
ND2	24	4.833	0.005	11	0.974	-4.714	-1.841*
G3PDH	10	1.287	0.003	5	0.460	0.711	-1.552
MUSK	3	0.843	0.002	4	0.655	-0.141	0.178

S : number of segregating sites; k : number of nucleotide differences; π : nucleotide diversity; h : number of haplotypes; Hd : haplotype diversity; D : Tajima's D ; F_s : Fu's F_s .

Our data recovered high values of segregating sites (S), nucleotide differences (k), haplotype diversity (Hd) and low values of nucleotide diversity (π) were obtained for both subspecies (excepted for *M. f. ferrugineus* in G3PDH). Neutrality tests showed signs of population fluctuations for *M. f. ferrugineus* and *M. f. elutus*. Values of Fu's F_s statistic were significantly negative in ND2 and significantly positive in G3PDH for *M. f. ferrugineus*. On the other hand, Tajima's D was significantly

negative in ND2 and G3PDH for *M. f. ferrugineus*, and in ND2 for *M. f. elutus*. Genetic distances (uncorrected *p*-distance) are shown in Table 3.

Table 3 List of the uncorrected *p*-distance values within and among subspecies.

<i>Genus/uncorrected-p</i>			
<i>distance</i>	<i>M. f. elutus</i>	<i>M. f. ferrugineus</i>	<i>M. f. elutus/M. f. ferrugineus</i>
CYTB			
within populations	0.003	0.004	-
among populations	-	-	0.031
ND2			
within populations	0.005	0.003	-
among populations	-	-	0.036
G3PDH			
within populations	0.001	0.001	-
among populations	-	-	0.001
MUSK			
within populations	0	0.001	-
among populations	-	-	0.007

Phylogenetic analysis

The Bayesian Inference analysis based on the concatenated dataset (3051 bp, CYTB, ND2, MUSK, and G3PDH) strongly support the monophyly of *M. ferrugineus* with respect to the outgroup (Figure 2). Within *M. ferrugineus*, two well supported major clades were recognized, fully agreeing with subspecific limits. One lineage consisted of the *M. f. ferrugineus* population from the Guiana shield (north of the Amazon), whereas the second lineage included *M. f. elutus* specimens from Madeira-Tapajós interfluvium, south of the Amazon (Figure 2). Beyond the high support for the reciprocal monophyly of both subspecies, the relationships within each taxon did not receive strong statistical support ($pp < 0.95$).

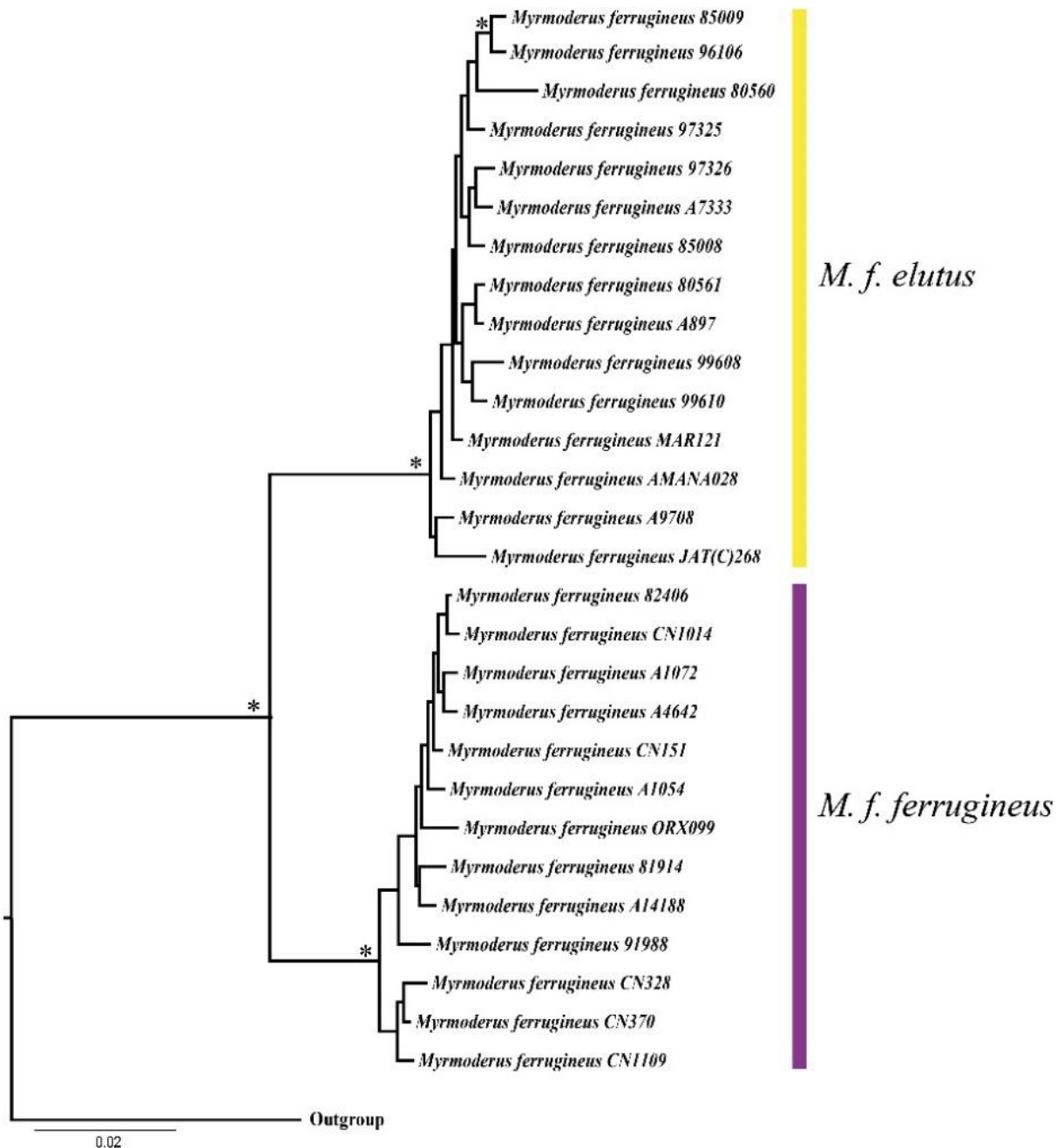


Figure 2 Bayesian phylogeny based on the concatenated dataset showing the relationships among phylogroups of *M. ferrugineus*. Populations north (*M. f. ferrugineus*; in purple) and south (*M. f. elutus*) of the Amazon River were recovered as reciprocally monophyletic. Asterisks correspond to the nodes with strong statistical support (posterior probability, pp=1.0).

We estimated a species tree for *M. ferrugineus* and *M. squamosus* (the nearest outgroup for which sequences from all sampled genes were available) using four independent loci (CYTB, ND2, G3PDH and MUSK). Both the monophyly of *M. ferrugineus* as well as that of its subspecies (*M. f. ferrugineus* and *M. f. elutus*) received high statistical support (pp = 1.0, data not shown). The

divergence times revealed an initial divergence of *M. ferrugineus* and *M. squamosus* at around ~90 split between *M. f. ferrugineus* and *M. f. elutus* was estimated as having taken place during the Holocene (~5 Kya, CI = 2.5 - 7.5 kya, Figure 3).

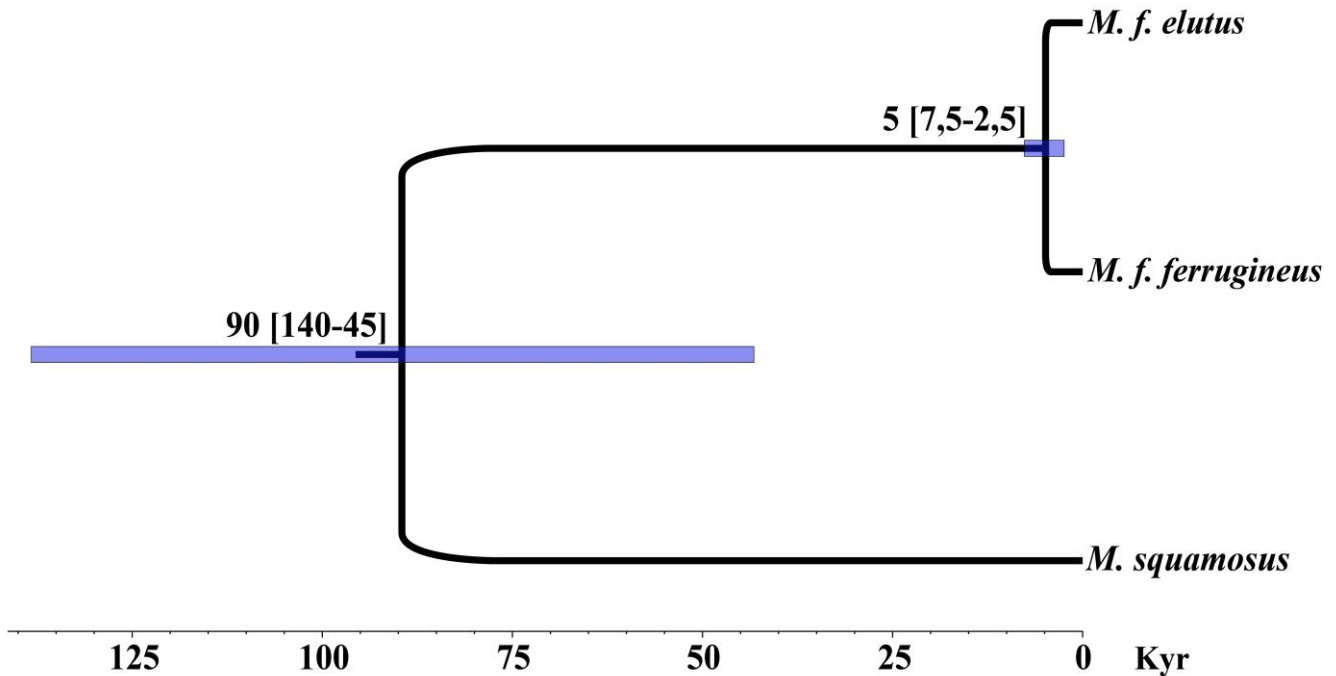


Figure 3 Species tree of *M. ferrugineus* clades and related outgroup *M. squamosus* based on all genes sequenced, constructed using *BEAST. Divergence times is shown to the left of nodes. The time scale shows time from past to present (left to right) in thousands of years ago. Bars show 95% credible intervals around estimates of the mean time to the most recent common ancestor (TMRCA).

Population structure, gene flow and demography

The median-joining haplotype networks based on CYTB, ND2 and MUSK sequences recovered the same two phylogroups (*M. f. ferrugineus* and *M. f. elutus*) that were already identified in phylogenetic analyses. These clades display non-overlapping geographic distributions and are separated by large numbers of mutational steps (Figure 4). However, G3PDH recovered no population structure.

IMa2 analyses favored scenarios of absence of gene flow among populations of *M. f. ferrugineus* and *M. f. elutus*. Migration events were rejected by LRT tests among most pairwise comparisons. According to this analysis, the split between *M. f. ferrugineus* and *M. f. elutus* was centered in the Holocene, but could have started at ca. 75 kya, during the Late Pleistocene (Table 3).

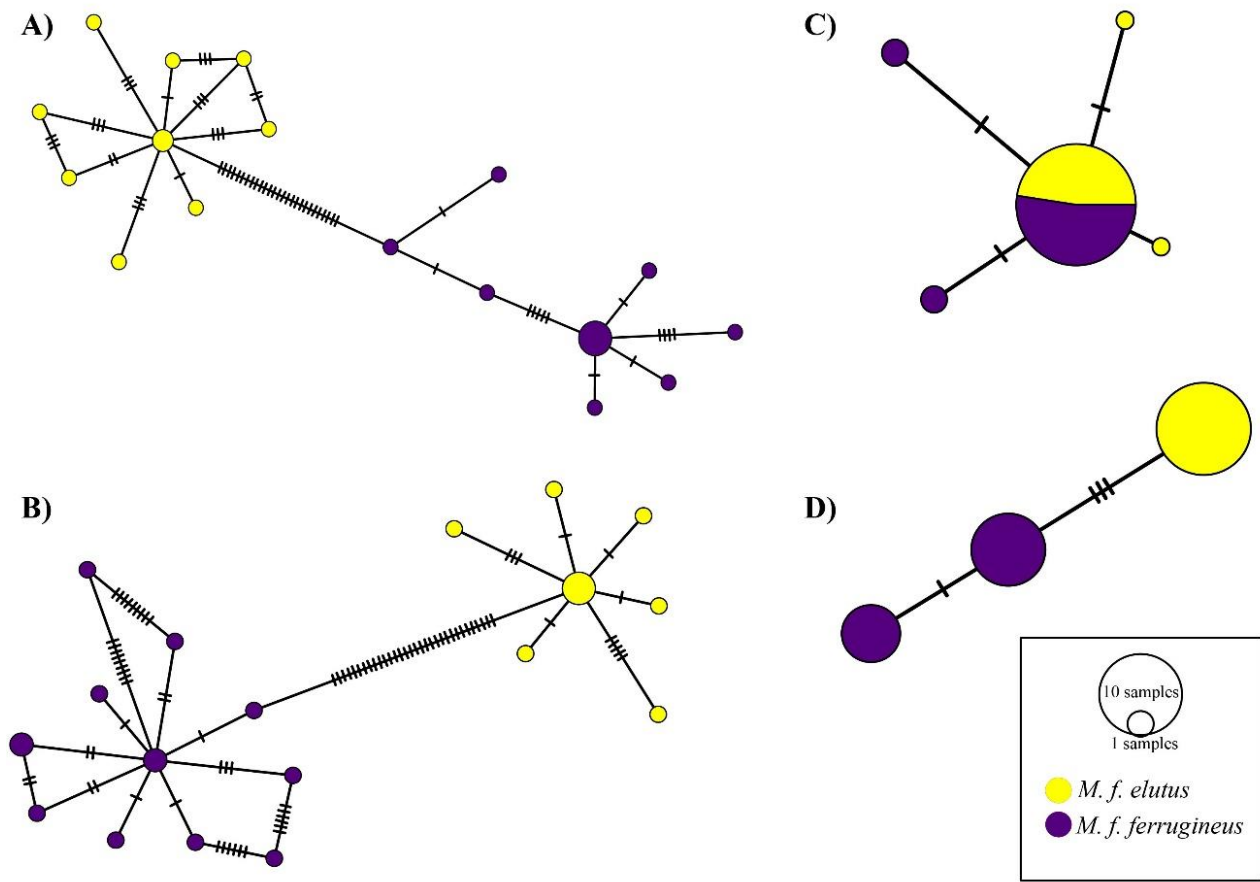


Figure 4 Median-joining statistical networks based on: A) CYTB; B) ND2; C) G3PDH; D) MUSK. Each circle represents a haplotype and its size is proportional to its total frequency (see legend). Branches and black crossbars represent a single nucleotide change.

Table 3 Summary of the IMa2 results between *M. ferrugineus* populations north (*M. f. ferrugineus*) and south (*M. f. elutus*) of the Amazon River (for more details, see text).

Geographical pairs	m1*	m2*	t [†]	t [†] (HPD90Lo)	t [†] (HPD90Hi)
<i>M. f. ferrugineus</i> / <i>M. f. elutus</i>	0.57	0	3.487	2.663	74.960

*Population migration rate ($q1 \times m1/2$) on the coalescent (e.g. $m1$ = rate of migration from population 2 to population 1).

[†]Time of population splitting in years (t/u).

The Extend Bayesian skyline plots (EBSP) simulated population dynamics over time for both *M. f. ferrugineus* and *M. f. elutus*. While *M. f. ferrugineus* presents a clear pattern of population

increase during the last one thousand years (Kya), *M. f. elutus* shows population stability between 200 and 800 Kya, with a gradual population expansion recovered over the last 200 Kya (Figure 5).

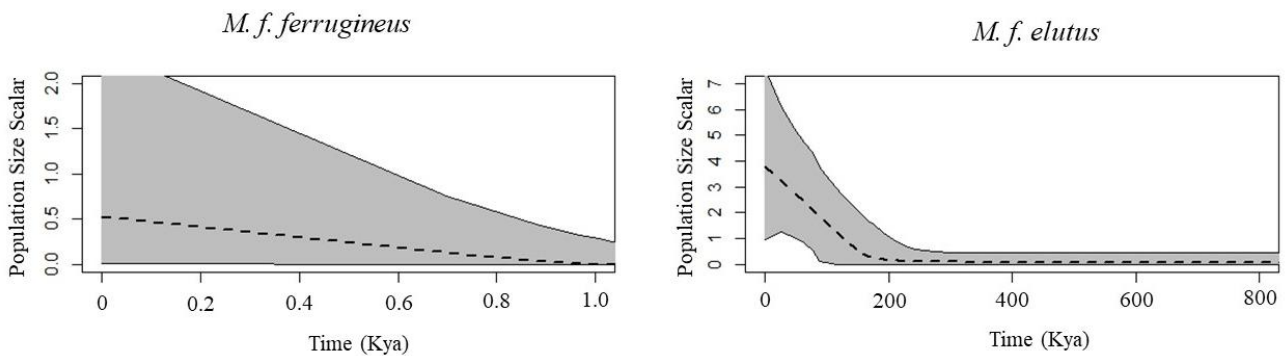


Figure 5 The Extended Bayesian skyline plots (EBSP) for *M. f. ferrugineus* and *M. f. elutus* based on all genes sequenced. The dashed line in the EBSP is the median estimated population size and solid lines are the 95% credible interval. The x-axis corresponds to time in thousand years before present while the y-axis is logarithmic.

DISCUSSION

Intraspecific relationships in *M. ferrugineus*

The subspecies *M. f. ferrugineus* and *M. f. elutus* are relatively homogeneous in morphology and coloration (Zimmer & Isler, 2003). Nevertheless, the Bayesian Inference analysis based on the concatenated dataset recovered two reciprocally monophyletic, strongly supported, lineages within *M. ferrugineus* corresponding to the recognized subspecies: *M. f. ferrugineus* and *M. f. elutus* (Figure 2). The same result was also found in the haplotype networks based on CYTB, ND2 and MUSK (Figure 4).

Our results demonstrated a deep and strong genetic divergence within *M. ferrugineus*, suggesting that the low phenotypic diversity in *M. ferrugineus* may obscure cryptic species-level diversity, as also verified for other Amazonian upland terra-firme bird taxa (Fernandes et al. 2012, Batista et al. 2013, Rodrigues et al. 2013). However, given their recent divergence time (estimates converge into the Holocene), it is possible that, if in contact, *M. f. ferrugineus* and *M. f. elutus* would interbreed freely. Pulido-Santacruz et al. (2018) demonstrated for an Amazonian antbird species complex that phenotypically cryptic lineages isolated by 3-5 million years have already acquired significant post-zygotic reproductive incompatibilities, but levels of reproductive isolation are unknown for taxa diverging for less than 1 million years such as *M. ferrugineus* taxa. Therefore, despite the observed genetic divergence *M. f. ferrugineus* and *M. f. elutus*, we refrain from splitting these phenotypically differentiated taxa as separate species and would rather treat them as divergent and structured phylogroups. Future studies should address in detail whether vocal differences

observed between *M. f. ferrugineus* and *M. f. elutus* (see above) are significant and diagnostic between them.

The Amazon as a barrier to geneflow for antbirds

The Ferruginous-backed Antbird walks constantly over the forest floor, hopping up on to and walking along logs, sometimes hopping or walking up through branches of fallen trees (Zimmer & Isler, 2003; personal observations). According to Smith et al. (2014), understory species would have more diversity than species inhabiting the canopy, as physiognomy and more balanced distribution of food resources within canopy species would be responsible for the greater dispersal ability. Therefore, species that fly long distances would not present an accumulation of genetic diversity, assuming the lineage persists over evolutionary timescales. Moore et al. (2008) also calculated the dispersal success rate versus distance in seven different families of birds. In four species of *Thamnophilidae* antbirds (*Myrmotherula fulviventris*, *Myrmeciza exsul*, *Hylophylax naevioides* and *Thamnophilus atrinucha*), Moore et al. (2008) showed that the success rates of dispersals over 300m were null, concluding that there is an inverse correlation between distance and the likelihood of successful dispersion (chances of success decrease with increasing distances). Similar result was also presented by Awade et al. (2017).

The identification of two distinct lineages within *M. ferrugineus*, i.e., *M. f. ferrugineus* and *M. f. elutus*, and the lack of migrants between the two populations reinforce the role of the Amazon River as a geographical barrier (Figures 2 and 4). Recent studies have shown that in fact rivers can act as barriers for different lineages, but this cannot be generalized. For example, populations of *Xenops minutus* (Aves: Furnariidae) presented gene flow across the Negro and Xingu rivers in Amazonia (Harvey & Brumfield, 2015). Another example was reported for the snake *Bothrops atrox*, where populations separated by Amazon and Tapajós rivers diverged recently, but also experienced low but symmetrical levels of gene flow across these rivers (Gibbs et al., 2018). As presented by Harvey & Brumfield (2015) and Gibbs et al. (2018), our results also suggest that although the Amazon is not an absolute barrier to gene flow, the river can significantly prevent migration and interaction between the two populations of sister taxa.

The riverine barrier hypothesis has influenced biogeographic studies based on different Amazonian taxa and this is probably the most widely tested hypothesis of diversification within the biome. However, it is known that the diversification within Amazonia is extremely complex, but cannot be explained from a single perspective (Haffer, 1985; Hoorn et al., 2011; Latrubesse et al., 2010; Santos et al., 2009; Smith et al., 2014; Wang et al., 2017). Our results, nonetheless confirm that major Amazonian rivers can be correlated with the generation and maintenance of genetic diversity for some species at least. The strong genetic division between *M. f. ferrugineus* and *M. f. elutus* is clearly correlated with the presence of Amazon River. However, our results regarding the timing of

divergence showed that the formation of the Amazon River itself was probably not responsible for the separation of the lineages. According to the results of BEAST and IMA2, the possible dating for divergence between *M. f. ferrugineus* and *M. f. elutus* spanned the past 75 ky and was apparently centered in the Holocene (Figure 3; Table 3). The main studies on paleogeography, paleoecology and stratigraphy of the Amazon river showed temporal scales much older than those presented for the separation between *M. f. ferrugineus* and *M. f. elutus*. According to Hoorn et al. (2010), the establishment of the Amazon River would have occurred around 7 million years ago (Ma). Alternatively, Latrubesse et al. (2010) postulated that the river would have originated around 6.5 to 5 Ma. Finally, Campbell et al. (2006) attributed a more recent date for the formation of the Amazon River, around 2.5 Ma.

A recent dispersal across the Amazon River explains *M. ferrugineus* phylogeographic structure

The pattern of isolation of *M. f. ferrugineus* and *M. f. elutus* is consistent with previous studies, supporting the importance of the Amazon River as a driver of diversification (Gibbs et al., 2018; Hoorn et al., 2010). However, our results showed that as early as the Late Pleistocene and the Holocene, some *M. f. ferrugineus* individuals somehow crossed or were transferred across the Amazon River. As a result, two distinct population were then defined, one on the Guiana shield (*M. f. ferrugineus*) and another in Madeira-Tapajós interfluve (*M. f. elutus*).

Punyasena et al. (2008) proposed that the middle Holocene was an important period of precipitation change, from previously drier conditions to more humid ones as in the present Holocene, with more stable temperatures. According to Cheng et al. (2013), based on results from speleothem oxygen isotope records, which revealed a large-scale decrease in $\delta^{18}\text{O}$ values from the LGM to the early-mid Holocene, drastic climatic changes from severely dry to substantially more humid took place in northeastern Brazil and eastern Amazonia. Similar results were presented by Wang et al. (2017), in relation to rainfall levels in Amazonia in the last 45,000 years. Compared to modern levels, precipitation in the region was lower during the last glacial maximum (about 21,000 years ago) but higher in the middle of the Holocene (about 6,000 years ago).

In addition to the climatic factors in the Holocene, several authors have suggested important geomorphic changes in the Solimões-Amazon rivers during the Late Pleistocene and Holocene. According to Passos et al. (2013), the most striking changes in the channels of the Solimões and Amazon rivers are associated with geomorphological changes caused by the deposition and erosion processes. Passos et al. (2013) showed that the characteristics of the depositional morphology of the fluvial terraces are indicative of a meandering fluvial style during the Pleistocene and part of the Holocene, differently from the current fluvial anastomosed style.

According to Gonçalves Júnior et al. (2016), since the Middle Holocene to nowadays, the gradual conversion of the meandering system into the current anabranching systems took place, due to the increase of the regional water base level caused by the sea level rise from the Late Pleistocene to the Middle Holocene. This probably also led to the expansion of *várzea* seasonally flooded forests along river banks, possibly replacing unflooded *terra firme* forests. As verified nowadays for several western Amazonian tributaries such as the Purus, Jurua, Beni, Ucayali, and Pastaza rivers, an intense meandering system leads to frequent lateral river migration of pieces of land across river banks (Latrubesse et al. 2015). The sinuosity present in the Amazon River during the Late Pleistocene would reach its end by the mid-Holocene with the implementation of an anabranching fluvial system, and probably with the expansion of seasonally flooded vegetation types in replacement of upland vegetation types along the main river course. Therefore, lateral river migration and proximity of unflooded forests to the river channel could have facilitated the transfer of *M. ferrugineus* individuals across the mid-Amazon River before the Holocene. In contrast, the raise of water level basin and the ensuing establishment of anabranching system by the mid-Holocene would act as a geographical barrier isolating *M. f. ferrugineus* and *M. f. elutus*, whose effect was probably magnified by the expansion of flooded vegetation types along the river's course, which are not occupied by the species. Our most likely time estimates for the split of *M. f. ferrugineus* and *M. f. elutus* are strikingly concordant with the pattern of Late-Pleistocene - Holocene drainage evolution for the Amazon River supported by Passos et al (2013) and Gonçalves Junior et al. (2016).

REFERENCES

- Aleixo, A. (2004) Historical diversification of a terra-firme forest bird superspecies: A phylogeographic perspective on the role of different hypotheses of amazonian diversification. *Evolution*, **58**, 1303–1317.
- Alfaro, J. W. L., Boubli, J. P., Paim, F. P., Ribas, C. C., da Silva, M. N. F., Messias, M. R., ... & Pinho, G. M. (2015) Biogeography of squirrel monkeys (genus *Saimiri*): South-central Amazon origin and rapid pan-Amazonian diversification of a lowland primate. *Molecular phylogenetics and evolution*, **82**, 436–454.
- Antonelli, A., Quijada-mascareñas, A., Crawford, A.J., John, M., Velazco, P.M., & Wüster, W. (2009) Molecular studies and phylogeography of Amazonian tetrapods and their relation to geological and climatic models. 386–404.
- Awade, M., Candia-Gallardo, C., Cornelius, C., & Metzger, J. P. (2017) High emigration propensity and low mortality on transfer drives female-biased dispersal of *Pyrgilena leucoptera* in fragmented landscapes. *PloS one*, **12**, e0170493.
- Campbell, K.E., Frailey, C.D., & Romero-Pittman, L. (2006) The Pan-Amazonian Ucayali Penneplain, late Neogene sedimentation in Amazonia, and the birth of the modern Amazon River system. *Palaeogeography, Palaeoclimatology, Palaeoecology*, **239**, 166–219.
- Cheng, H., Sinha, A., Cruz, F. W., Wang, X., Edwards, R. L., d’Horta, F. M., Ribas, C., Vuille, M., Stott, L. D. & Auler, A. S. (2013) Climate change patterns in Amazonia and biodiversity. *Nature communications*, **4**, 1411.
- Drummond, A. J., & Rambaut, A. (2007) BEAST: Bayesian evolutionary analysis by sampling trees. *BMC evolutionary biology*, **7**, 214.
- Drummond, A. J., Suchard, M. A., Xie, D., & Rambaut, A. (2012) Bayesian phylogenetics with BEAUti and the BEAST 1.7. *Molecular biology and evolution*, **29**, 1969–1973.
- Fu, Y. X. (1997) Statistical tests of neutrality of mutations against population growth, hitchhiking and background selection. *Genetics*, **147**, 915–925.
- Funk, W. C., Caldwell, J. P., Peden, C. E., Padial, J. M., De la Riva, I., & Cannatella, D. C. (2007) Tests of biogeographic hypotheses for diversification in the Amazonian forest frog, *Physalaemus petersi*. *Molecular phylogenetics and evolution*, **44**, 825–837.
- Gibbs, H.L., Sovic, M., Amazonas, D., Chalkidis, H., Valenzuela, D.S., & Moura-da-silva, A.N.A.M. (2018) Recent lineage diversification in a venomous snake through dispersal across the Amazon River. 1–15.
- Gonçalves Júnior, E.S., Soares, E.A.A., Tatum, S.H., Yee, M., & Mittani, J.C.R. (2016) Pleistocene-Holocene sedimentation of Solimões-Amazon fluvial system between the tributaries Negro and

- Madeira, Central Amazon. *Brazilian Journal of Geology*, **46**, 167–180.
- Haffer, J. (1969) Speciation in Amazonian forest birds. *Science*, **165**(3889), 131–137.
- Hall, T. A. (1999) Bioedit: a user friendly biological sequence alignment editor Analysis Program for Windows 95/98/Nt. *Nucleic Acids Symposium Series*, **41**, 95–98.
- Harvey, M.G. & Brumfield, R.T. (2015) Genomic variation in a widespread Neotropical bird (*Xenops minutus*) reveals divergence, population expansion, and gene flow. *Molecular Phylogenetics and Evolution*, **83**, 305–316.
- Hasegawa, M., Kishino, H., & Yano, T. A. (1985) Dating of the human-ape splitting by a molecular clock of mitochondrial DNA. *Journal of molecular evolution*, **22**, 160–174.
- Heled, J., & Drummond, A. J. (2008) Bayesian inference of population size history from multiple loci. *BMC Evolutionary Biology*, **8**, 289.
- Hey, J., & Nielsen, R. (2004) Multilocus methods for estimating population sizes, migration rates and divergence time, with applications to the divergence of *Drosophila pseudoobscura* and *D. persimilis*. *Genetics*, **167**, 747–760.
- Hey, J. (2009) Isolation with migration models for more than two populations. *Molecular biology and evolution*, **27**, 905–920.
- Horn, C., Wesselingh, F.P., Ter Steege, H., Bermudez, M.A., Mora, A., Sevink, J., Sanmartín, I., Sanchez-Meseguer, A., Anderson, C.L., Figueiredo, J.P., Jaramillo, C., Riff, D., Negri, F.R., Hooghiemstra, H., Lundberg, J., Stadler, T., Särkinen, T., & Antonelli, A. (2010) Amazonia through time: Andean uplift, climate change, landscape evolution, and biodiversity. *Science*, **330**, 927–931.
- Kaefer, I. L., Tsuji-Nishikido, B. M., & Lima, A. P. (2012) Beyond the river: underlying determinants of population acoustic signal variability in Amazonian direct-developing *Allobates* (Anura: Dendrobatoidea). *Acta Ethologica*, **15**, 187–194.
- Kumar, S., Stecher, G., & Tamura, K. (2016) MEGA7: molecular evolutionary genetics analysis version 7.0 for bigger datasets. *Molecular biology and evolution*, **33**, 1870–1874.
- Lanfear, R., Calcott, B., Ho, S. Y., & Guindon, S. (2012) PartitionFinder: combined selection of partitioning schemes and substitution models for phylogenetic analyses. *Molecular biology and evolution*, **29**, 1695–1701.
- Latrubesse, E.M., Cozzuol, M., da Silva-Caminha, S.A.F., Rigsby, C.A., Absy, M.L., & Jaramillo, C. (2010) The Late Miocene paleogeography of the Amazon Basin and the evolution of the Amazon River system. *Earth-Science Reviews*, **99**, 99–124.
- Lavergne, A., Ruiz-García, M., Catzeflis, F., Lacote, S., Contamin, H., Mercereau-Puijalon, O., ... & De Thoisy, B. (2010) Phylogeny and phylogeography of squirrel monkeys (genus *Saimiri*) based on cytochrome b genetic analysis. *American Journal of Primatology*, **72**, 242–253.

- Leigh, J. W., & Bryant, D. (2015) Popart: full-feature software for haplotype network construction. *Methods in Ecology and Evolution*, **6**, 1110–1116.
- Librado, P., & Rozas, J. (2009) DnaSP v5: a software for comprehensive analysis of DNA polymorphism data. *Bioinformatics*, **25**, 1451–1452.
- Milliman, J. D., Steele, J. H., Thorpe, S. A., & Turekian, K. K. (2001) *River inputs*.
- Moore, R. P., Robinson, W. D., Lovette, I. J., & Robinson, T. R. (2008) Experimental evidence for extreme dispersal limitation in tropical forest birds. *Ecology letters*, **11**, 960–968.
- Nielsen, R., & Wakeley, J. (2001) Distinguishing migration from isolation: a Markov chain Monte Carlo approach. *Genetics*, **158**, 885–896.
- Nei, M. (1987) *Molecular evolutionary genetics*. Columbia university press.
- Passos, M. S., Soares, E. A. A., & Salazar, C. A. (2013) Análise bitemporal do Rio Solimões no trecho entre Manacapuru e Manaus (Amazônia Central) por meio de imagens Landsat-5/TM. *Simpósio Brasileiro de Sensoriamento Remoto (SBSR)*, **16**, 3627–3634.
- Punyasena, S.W., Mayle, F.E., & McElwain, J.C. (2008) Quantitative estimates of glacial and Holocene temperature and precipitation change in lowland Amazonian Bolivia. *Geology*, **36**, 667–670.
- Rambaut, A., Drummond, A. J., & Suchard, M. (2007) Tracer v1. 6 <http://beast.bio.ed.ac.uk>. Tracer (visited on 2017-06-12).
- Ribas, C.C., Aleixo, A., Nogueira, A.C.R., Miyaki, C.Y., & Cracraft, J. (2012) A palaeobiogeographic model for biotic diversification within Amazonia over the past three million years. *Proceedings of the Royal Society B: Biological Sciences*, **279**, 681–689.
- Ronquist, F., Teslenko, M., Van Der Mark, P., Ayres, D. L., Darling, A., Höhna, S., ... & Huelsenbeck, J. P. (2012) MrBayes 3.2: efficient Bayesian phylogenetic inference and model choice across a large model space. *Systematic biology*, **61**, 539–542.
- Santos, J.C., Coloma, L.A., Summers, K., Caldwell, J.P., Ree, R., & Cannatella, D.C. (2009) Amazonian amphibian diversity is primarily derived from late Miocene Andean lineages. *PLoS Biology*, **7**, 0448–0461.
- Smith, B.T., McCormack, J.E., Cuervo, A.M., Hickerson, M.J., Aleixo, A., Cadena, C.D., Pérez-Emán, J., Burney, C.W., Xie, X., Harvey, M.G., Faircloth, B.C., Glenn, T.C., Derryberry, E.P., Prejean, J., Fields, S., & Brumfield, R.T. (2014) The drivers of tropical speciation. *Nature*, **515**, 406–409.
- Stephens, M., Smith, N. J., & Donnelly, P. (2001) A new statistical method for haplotype reconstruction from population data. *The American Journal of Human Genetics*, **68**, 978–989.
- Stephens, M., & Scheet, P. (2005) Accounting for decay of linkage disequilibrium in haplotype inference and missing-data imputation. *The American Journal of Human Genetics*, **76**, 449–462.

- Tajima, F. (1989) Statistical method for testing the neutral mutation hypothesis by DNA polymorphism. *Genetics*, **123**, 585-595.
- Thompson, J. D., Higgins, D. G., & Gibson, T. J. (1994) CLUSTAL W: improving the sensitivity of progressive multiple sequence alignment through sequence weighting, position-specific gap penalties and weight matrix choice. *Nucleic acids research*, **22**, 4673–4680.
- Wallace, A. R. (1854) On the monkeys of the Amazon. *Annals and Magazine of Natural History*, **14**, 451–454.
- Wang, X., Edwards, R.L., Auler, A.S., Cheng, H., Kong, X., Wang, Y., Cruz, F.W., Dorale, J.A., & Chiang, H.W. (2017) Hydroclimate changes across the Amazon lowlands over the past 45,000 years. *Nature*, **541**, 204–207.
- Weir, J. T., & Schluter, D. (2008) Calibrating the avian molecular clock. *Molecular ecology*, **17**, 2321–2328.
- Zimmer, K. J., & Isler, M. L. (2003) Family Thamnophilidae (typical antbirds). *Handbook of the birds of the world*, **8**, 448–681.

APPENDIX

Appendix S1

Museum	Tissue number	Species	Subspecies	Locality
MPEG	CN1014	<i>M. ferrugineus</i>	<i>ferrugineus</i>	REBIO Maicuru, Almerim, Pará
MPEG	CN151	<i>M. ferrugineus</i>	<i>ferrugineus</i>	FLOTA of Faro, 70km NW of Faro, Pará
MPEG	CN1109	<i>M. ferrugineus</i>	<i>ferrugineus</i>	FLOTA of Paru, Almerim, Pará
MPEG	CN328	<i>M. ferrugineus</i>	<i>ferrugineus</i>	FLOTA of Trombetas, Óbidos, Pará
MPEG	CN370	<i>M. ferrugineus</i>	<i>ferrugineus</i>	ESEC Grão-Pará, Alenquer, Pará
MPEG	ORX099	<i>M. ferrugineus</i>	<i>ferrugineus</i>	Rio Xingu, Faro, Vila de Maracanã, Pará
INPA	A14188	<i>M. ferrugineus</i>	<i>ferrugineus</i>	Left bank of Negro river, Parque Nacional Anavilhanas, Amazonas
INPA	A1072	<i>M. ferrugineus</i>	<i>ferrugineus</i>	Parque Nacional Viruá, Caracaraí, Roraima
INPA	A4642	<i>M. ferrugineus</i>	<i>ferrugineus</i>	Right bank of Jatapú river, São Sebastião Uatumã, Amazonas
INPA	A1054	<i>M. ferrugineus</i>	<i>ferrugineus</i>	Parque Nacional Viruá, Caracaraí, Roraima
MZUSP	81914	<i>M. ferrugineus</i>	<i>ferrugineus</i>	RESEX Cajari, Vila Marinho, Amapá
MZUSP	82406	<i>M. ferrugineus</i>	<i>ferrugineus</i>	Vila Nova, Macapá, Amapá
MZUSP	91988	<i>M. ferrugineus</i>	<i>ferrugineus</i>	RESEX Cajari, Vila Marinho, Amapá
MPEG	JAT(C)268	<i>M. ferrugineus</i>	<i>elutus</i>	Left bank of Tapajós river, Jatobá, Pará
MPEG	AMANA028	<i>M. ferrugineus</i>	<i>elutus</i>	Right bank of Igarapé Porquinho, Garimpo JMS, FLONA Amanã, Itaituba, Pará
MPEG	MAR121	<i>M. ferrugineus</i>	<i>elutus</i>	Km 137 of Estrada do Estranho, Manicoré, Pará
INPA	A9708	<i>M. ferrugineus</i>	<i>elutus</i>	Left bank of Tapajós river, Itaituba, Pará
INPA	A897	<i>M. ferrugineus</i>	<i>elutus</i>	Left bank of Uatamã, Matatá, Amazonas

Museum	Tissue number	Species	Subspecies	Locality
INPA	A7333	<i>M. ferrugineus</i>	<i>elutus</i>	Left bank of Tapajós river, Vila Raiol, Pará
MZUSP	80561	<i>M. ferrugineus</i>	<i>elutus</i>	Roosevelt river, Amazonas
MZUSP	99608	<i>M. ferrugineus</i>	<i>elutus</i>	UHE Tabajara, right bank of Ji-Paraná, Machadinho d'Oeste, Rondônia
MZUSP	99610	<i>M. ferrugineus</i>	<i>elutus</i>	UHE Tabajara, right bank of Ji-Paraná, Machadinho d'Oeste, Rondônia
MZUSP	85008	<i>M. ferrugineus</i>	<i>elutus</i>	Br-230, Jacareacanga, Pará
MZUSP	97325	<i>M. ferrugineus</i>	<i>elutus</i>	Right bank of Sucunduri river, Amazonas
MZUSP	97326	<i>M. ferrugineus</i>	<i>elutus</i>	Right bank of Sucunduri river, Amazonas
MZUSP	80560	<i>M. ferrugineus</i>	<i>elutus</i>	Roosevelt river, Amazonas
MZUSP	85009	<i>M. ferrugineus</i>	<i>elutus</i>	Br-230, Jacareacanga, Pará
MZUSP	96106	<i>M. ferrugineus</i>	<i>elutus</i>	Left bank of Sucunduri river, Amazonas
MPEG	SC077	<i>M. squamosus</i>	-	Sítio Paraíso, Vila Itoupava, Blumenau, Santa Catarina
MPEG	SC078	<i>M. squamosus</i>	-	Sítio Paraíso, Vila Itoupava, Blumenau, Santa Catarina
LSUMZ	B16940	<i>M. squamosus</i>	-	São Paulo
LSUMZ	B93476	<i>M. eowilsoni</i>	-	Flor de Cafe, San Martin, Peru
LSUMZ	B93477	<i>M. eowilsoni</i>	-	Flor de Cafe, San Martin, Peru
FMNH	FMNH399262	<i>M. ruficaudus</i>	-	Ibateouara, Alagoas
FMNH	FMNH392445	<i>M. ruficaudus</i>	-	Serra of Espelho, Pernambuco
LGEMA	LGEMA1527	<i>M. ruficaudus</i>	-	Ribeirão do Largo, Bahia
MZUSP	85433	<i>M. loricatus</i>	-	Mariana, Minas Gerais
MZUSP	85430	<i>M. loricatus</i>	-	Mariana, Minas Gerais
MZUSP	RBO835	<i>M. loricatus</i>	-	São Paulo
ZMCU	S1062	<i>M. loricatus</i>	-	São Paulo

Appendix S2

Gene	Primers	Sequences (5' - 3')	References
Cytochrome b (CYTB)	L14841	AAC TGC AGT CAT CTC CGG TTT ACA AGA C	Kocher et al. (1989)
Cytochrome b (CYTB)	H16065	AAC TGC AGT CAT CTC CGG TTT ACA AGA C	Sorenson et al. (1999)
NADH dehidrogenase 2 (ND2)	L5215	TAT CGG GCC CAT ACC CCG AAA T	Hackett (1996)
NADH dehidrogenase 2 (ND2)	H6313	CTC TTA TTT AAG GCT TTG AAG GC	Sorenson et al. (1999)
Glyceraldehyde 3-phosphate dehydrogenase intron 11 (G3PDH)	G3P-13b	TCC ACC TTT GAT GCG GGT GCT GGC AT	Fjeldså et al. (2003)
Glyceraldehyde 3-phosphate dehydrogenase intron 11 (G3PDH)	G3P-14b	AAG TCC ACA ACA CGG TTG CTG TA	Fjeldså et al. (2003)
Muscle skeletal receptor tyrosine kinase (MUSK)	13F	CTT CCA TGC ACT ACA ATG GGA AA	Clark & Witt (2006)
Muscle skeletal receptor tyrosine kinase (MUSK)	13R	CTC TGA ACA TTG TGA TCC TCA A	Clark & Witt (2006)